Alkylation of Pyridinium Acceptors via Thermal and Photoinduced Electron Transfer in Charge-Transfer Salts with Organoborates

Dunming Zhu and Jay K. Kochi*

Department of Chemistry, University of Houston, Houston, Texas 77204-5641

Colored salts of pyridinium tetraalkylborates [**Py**$^+$,BR$_4^-$] are readily isolated by the metathesis of LiBMe$_4$, LiBMePh$_3$, or NaBPh$_4$ with a series of pyridinium triflates in aqueous solution. The interionic charge-transfer (CT) interaction between the organoborate anions and the pyridinium cations is established by their characteristic charge-transfer absorption bands and X-ray crystal structures. Thermal and photochemical CT activations of the salts lead to efficient methyl transfer from tetramethylborate (or methyltriphenylborate) to the pyridinium cations to afford the various nucleophilic adducts (**Py**-Me) in good yields. Contact charge-transfer ion pairs are identified as the critical intermediates in the formal nucleophilic addition and thus play important roles in determining the regiochemistry of the alkylation and the solid-state reactivity of the [**Py**$^+$,BR$_4^-$] salts.

Introduction

Organometalate salts (R$_n$M$^-$) are extensively utilized as nucleophilic sources of carbanionoid (R$^-$) ligands.[1,2] These reactions are conventionally formulated as simple nucleophilic processes, and the metal complex is regarded as a carrier for the nucleophilic (R$^-$) group. Organoborate salts exemplify these reagents, and the tetraalkylborates such as BMe$_4^-$ are sources of nucleophilic alkyl groups, just as borohydride is a source of hydride (H$^-$). As such, they represent mild and selective alternatives to Grignard and organolithium reagents in organic synthesis.[3,4] Organoborates have also been identified as one-electron reducing agents (electron donors) in a variety of thermal and photochemical redox processes.[5] A well-known example is alkyltriphenylborates serving as free radical initiators for the photopolymerization of acrylates,[6] in which the key steps involve an initial photoinduced electron transfer and subsequent boron−carbon cleavage of the boranyl in-

termediates, as demonstrated by time-resolved spectroscopic and trapping studies.[7,8] As such, the question arises as to what role the electron-donor property of the borate anion plays in the nucleophilic alkyl transfer. To address this question, we concentrate herein on the transfer of a methyl ligand from tetramethylborate and its substituted analogues. As cationic electrophiles, we have chosen the series of pyridinium cations (**Py**$^+$) in Chart 1, the electrophilic properties of which can be modulated by substitution of electron-donating or electron-withdrawing groups on the pyridine nucleus.[9] Since the nucleophilic group is anionic and the electrophiles in Chart 1 are positively charged, the specific *interionic* interactions can be pinpointed by the isolation and

(1) For some reviews, see: (a) Posner, G. H. *An Introduction to Synthesis Using Organocopper Reagents*; Wiley: New York, 1980. (b) Lipshutz, B. H.; Sengupta, S. In *Organic Reaction*; John Wiley & Sons: New York, 1992; Vol. 41, Chapter 2, pp 135−631. (c) Kauffmann, T. *Angew. Chem., Int. Ed. Engl.* **1996**, *35*, 386-403.

(2) For some recent leading papers, see: (a) Uchiyama, M.; Furumoto, S.; Saito, M.; Kondo, Y.; Sakamoto, T. *J. Am. Chem. Soc.* **1997**, *119*, 11425. (b) Uchiyama, M.; Koike, M.; Kameda, M.; Kondo, Y.; Sakamoto, T. *J. Am. Chem. Soc.* **1996**, *118*, 8733. (c) Lipshutz, B. H.; Woo, K.; Gross, T.; Buzard, D. J.; Tirado, R. *SYNLETT* **1997**, 477. (d) Kjonaas, R. A.; Hoffer, R. K. *J. Org. Chem.* **1988**, *53*, 4133. (e) Nakamura, E.; Mori, S.; Nakamura, M.; Morokuma, K. *J. Am. Chem. Soc.* **1997**, *119*, 4887. (f) Nakamura, E.; Mori, S.; Morokuma, K. *J. Am. Chem. Soc.* **1997**, *119*, 4900. (g) Inoue, R.; Shinokubo, H.; Oshima, K. *Tetrahedron Lett.* **1996**, *37*, 5377.

(3) (a) Negishi, E. *J. Organomet. Chem.* **1976**, *108*, 281. (b) Negishi, E.; Chin, K. W.; Yoshida, T. *J. Org. Chem.* **1975**, *40*, 1676. (c) Negishi, E.; Abramovitch, A.; Merrill, R. E. *J. Chem. Soc., Chem. Commun.* **1975**, 138.

(4) (a) Hunter, R.; Michael, J. P.; Tomlinson, G. D. *Tetrahedron* **1994**, *50*, 871. (b) Miyaura, N.; Itoh, M.; Suzuki, A. *Bull. Chem. Soc. Jpn.* **1977**, *50*, 2199. (c) Miyaura, N.; Itoh, M.; Suzuki, A. *Synthesis* **1976**, 618.

(5) Billing, R.; Rehorek, D.; Hennig, H. *Topics Curr. Chem.* **1990**, *158*, 151.

(6) (a) Eaton, D. F. *Pure Appl. Chem.* **1984,** *56*, 1191. (b) Gottschalk, P.; Schuster, G. B. U.S. Patent 4,772,541, 1988 (*Chem. Abstr.* **1987**, *107*, 187434n). (c) Gottschalk, P.; Neckers, D. C.; Schuster, G. B. U.S. Patent 4,772,530, 1988 (*Chem. Abstr.* **1987**, *107*, 187434n). (d) Farid, S. Y.; Moody, R. E. U.S. Patent 4,859,572, 1989 (*Chem. Abstr.* **1990**, *112*, 88310r). (e) Satomura, M.; Iwakura, K.; Igarashi, A. U.S. Patent 4,847,236, 1989 (*Chem. Abstr.* **1988**, *109*, 160719p). (f) Yamaguchi, J., Masaki, O.; Takanori, H. U.S. Patent 4,902,604, 1990 (*Chem. Abstr.* **1989**, *111*, 244332m). (g) Koike, M.; Kita, N. U.S. Patent 4,950,581, 1990 (*Chem. Abstr.* **1989**, *110*, 183030s). (h) Kawamura, K.; Okamoto, Y. U.S. Patent 4,971,891, 1990 (*Chem. Abstr.* **1989**, *111*, 222173h). (i) Shanklin, M. S.; Gottschalk, P.; Adair, P. C. U.S. Patent 5,055,372, 1991 (*Chem. Abstr.* **1992**, *116*, 265621y). (j) Marino, T.; DeRaaff, A. M.; Neckers, D. C. *Rad Tech 96' North Am. UV/ED Conf. Proc.* **1996**, 7. (k) Neckers, D. C.; Sarker, A. M.; Hassoon, S. A.; Polykarpov, A. Y.; DeRaaff, A. M.; Marino, T. L. PCT Int. Appl. WO 97 21,737, 1995 (*Chem. Abstr.* **1997**, *127*, 122109d). (l) For an early review, see: Dietliker, J. *Photochemical and Radiation Curing*; Oldring, P. K. T., Ed.; SITA: London, 1990.

(7) (a) Chatterjee, S.; Davis, P. D.; Gottschalk, P.; Kurz, M. E.; Sauerwein, B.; Yang, X.; Schuster, G. B. *J. Am. Chem. Soc.* **1990**, *112*, 6329. (b) Schuster, G. B. *Pure Appl. Chem.* **1990**, *62*, 1565. (c) Chrisope, D. R.; Schuster, G. B. *Organometallics* **1989**, *8*, 2737. (d) Chatterjee, S.; Davis, P. D.; Schuster, G. B.; Gottschalk, P. *J. Am. Chem. Soc.* **1988**, *110*, 2326.

(8) (a) Hassoon, S.; Sarker, A.; Polykarpov, A. Y.; Rodgers, M. A. J.; Neckers, D. C. *J. Phys. Chem.* **1996**, *100*, 12386. (b) Hassoon, S.; Sarker, A.; Rodgers, M. A. J.; Neckers, D. C. *J. Am. Chem. Soc.* **1995**, *117*, 11369. (c) Hassoon, S.; Neckers, D. C. *J. Phys. Chem.* **1995**, *99*, 9416. (d) Feng, K.; Zang, H.; Martin, D.; Marino, T. L.; Neckers, D. C. *J. Polym. Sci. (A)* **1998**, *36*, 1667. (e) Etter, M. C.; Holmes, B. N.; Kress, R. B.; Filipovich, G. *Isr. J. Chem.* **1985**, *25*, 264.
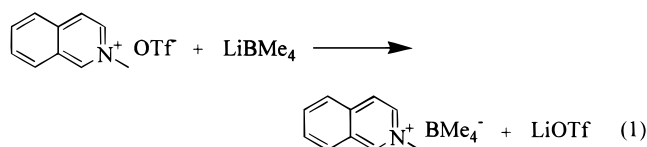
Chart 1
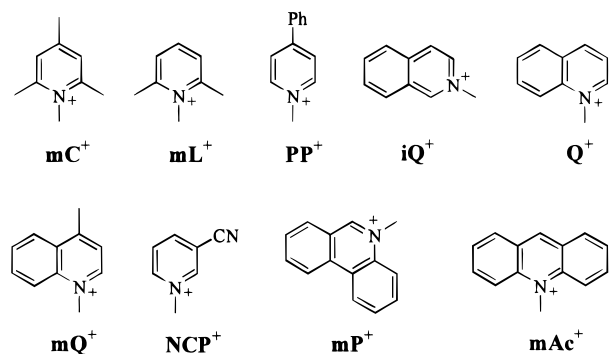
structural characterization of the pyridinium borate salts by X-ray crystallography.

Results

I. Synthesis of the Pyridinium Borate Salts. Upon the addition of lithium tetramethylborate to an aqueous solution of *N*-methylisoquinolinium triflate under an argon atmosphere, a bright yellow precipitate formed immediately. The precipitate was recrystallized by diffusion of diethyl ether into an acetonitrile solution at low temperature. The yellow needle crystals were freely soluble in acetonitrile, and ^{1}H NMR analysis showed only the characteristic resonances of the tetramethylborate anion and the *N*-methylisoquinolinium cation in a 1:1 ratio, i.e.,

Other tetramethylborate salts (**1**−**7**) were similarly prepared by metathesis with the pyridinium triflates in Chart 1, and the use of Li$^+$BMePh$_3^-$ or Na$^+$BPh$_4^-$ yielded the corresponding methyltriphenylborate (**8**−**12**) and tetraphenylborate (**13**−**17**) salts. The proton NMR spectra of these borate salts, as well as elemental analysis, confirmed the identity of these salts as simple unsolvated 1:1 electrolytes.

Several pyridinium borates were not stable upon storage at room temperature, even when carefully protected from air and light. For example, the yellow crystals of [**iQ**$^+$,BMe$_4^-$] (**4**) visibly darkened over the course of a few days to form a red-brown amorphous residue, and the lability discouraged the elemental analysis of the more unstable salts (**4**−**7**). An attempt to isolate the tetramethylborate salt of *N*-methylacridinium was unsuccessful, since the initially precipitated red-brown solid turned green within a minute of its preparation.[10]

Although the pyridinium triflate salts and the alkalimetal organoborates were colorless, the pyridinium
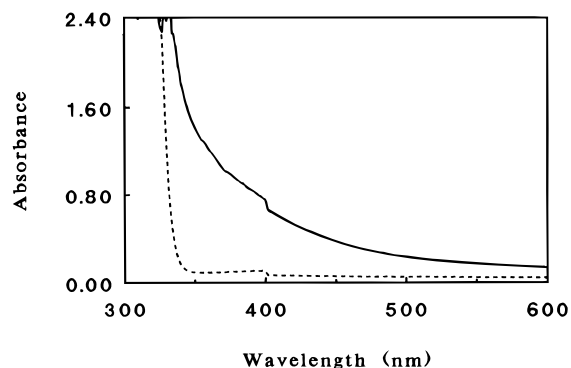
(9) (a) Bockman, T. M.; Cho, H.-C.; Kochi, J. K. *Organometallics* **1995**, *14*, 5221. (b) Bockman, T. M.; Kochi, J. K. *New J. Chem.* **1992**, *16*, 39. (c) Bockman, T. M.; Kochi, J. K. *J. Am. Chem. Soc.* **1989**, *111*, 4669. (d) Calderazzo, F.; Pampaloni, G.; Pelizzi, G.; Vitali, F. *Organometallics* **1988**, *7*, 1083.
(10) The green solid was identified as a mixture of *N,N*-dimethyl-9,9′-biacridanyl, bis(*N*-methylacridanyl)methane, 9,10-dimethylacridane, 9-methylacridane, and 9-methyl-10-acridanone.

Figure 1. Comparative UV−vis spectra of 4-phenylpyridinium tetramethylborate (—) and 4-phenylpyridinium triflate (- - -) in THF (0.005 M) showing the bathochromic shift of the end absorption due to the charge-transfer transition. [Note that TBA$^+$BMe$_4^-$ has no absorption beyond 300 nm.]

Table 1. UV−Vis Absorption Spectra of Charge-Transfer Salts in Solution and in the Crystalline Solid State[a]

acceptor	E(V vs SCE)[b]	BMe$_4^-$	BMePh$_3^-$	BPh$_4^-$
mC$^+$	1.63	371 (380)		
mL$^+$	1.45	387 (405)		
PP$^+$	1.27	470 (460)		
iQ$^+$	1.08	490 (490)	437 (400)	406
Q$^+$	0.90		470 (435)	418
NCP$^+$	0.83		485	485
mP$^+$	0.78		472 (445)	450
mAc$^+$	0.43		580	512

[a] The wavelength (nm) at 0.20 absorbance obtained from the diffuse reflectance spectrum in silica. Those obtained in THF solution are in parentheses. [b] Irreversible cathodic CV peak potential at 500 mV s^{-1}.

borates displayed colors that depended on both the cation and the anion. For the tetramethylborate salts, the colors of the crystals ranged from colorless (**mL**$^+$ and **mC**$^+$) to pale yellow (**PP**$^+$, **iQ**$^+$) to orange (**mP**$^+$). For each pyridinium cation, the yellow to orange color intensified in the order BPh$_4^-$ < BMePh$_3^-$ < BMe$_4^-$. *N*-Methylisoquinolinium tetraphenylborate, for example, was colorless, whereas the BMePh$_3^-$ and BMe$_4^-$ salts were pale yellow and bright yellow, respectively.

II. Charge-Transfer Spectra of the Pyridinium Borate Salts. UV−visible spectra of the salts **1**−**4** were measured in THF solution at −78 °C, and the charge-transfer bands appeared as spectral tails shown in Figure 1. The spectral positions were arbitrarily assessed as the wavelength at which the absorbance was 0.20, and the λ_{CT} values are summarized in Table 1. The CT absorbance exhibited a consistent red shift as the reduction potential of the cationic acceptor became less negative in the order **mC**$^+$ < **mL**$^+$ < **PP**$^+$ < **iQ**$^+$. [The absence of a corresponding low-energy absorption band in the spectrum of [**TBA**$^+$,BMe$_4^-$] was consistent with the limited electron affinity (i.e., high-energy LUMO) of the **TBA**$^+$ cation.] UV−visible spectra of salts **8**−**12** were measured at room temperature in THF solution, and they also showed a similar red shift as the reduction potential of the cationic acceptor became less negative (see Table 1). Since salts **13**−**17** were not soluble in THF (and only slightly soluble in acetonitrile), their UV−vis spectra were not evaluated.

The solid-state UV−visible spectra of salts **1**−**4** and **8**−**17** were measured as dilute mixtures in silica gel (0.1

mmol/g silica gel), in which the charge-transfer bands also appeared as spectral tails. The CT spectra (assessed as the wavelength at which the absorbance was 0.20 in Table 1) showed a consistent red shift of λ_{CT} as the reduction potential of the cationic acceptor increased in the order **mC$^+$** < **mL$^+$** < **PP$^+$** < **iQ$^+$** for BMe$_4^-$ and **iQ$^+$** < **Q$^+$** < **NCP$^+$** < **mP$^+$** < **Ac$^+$** for BMePh$_3^-$ and BPh$_4^-$ anions. A spectral blue shift was observed when the oxidation potential of the organoborate donors increased in the order tetramethylborate < methyltriphenylborate < tetraphenylborate.[11] Accordingly, these colored pyridinium salts of tetraalkylborates were identified as charge-transfer complexes, and the new UV−visible absorption was readily assigned to the charge-transfer transition in eq 2,

$$[\mathbf{Py}^+,\mathbf{BR}_4^-] \xrightarrow{h\nu_{CT}} [\mathbf{Py}^\bullet,\mathbf{BR}_4^\bullet] \qquad (2)$$

in which the cationic **Py$^+$** is the electron acceptor and the anionic tetraalkylborate is the electron donor, in accord with the Mulliken formulation of electron donor/acceptor interaction.[12] Similar charge-transfer transitions in the ion pair have also been observed in the 4,4′-bipyridinium salt of tetrakis[3,5-bis(trifluoromethyl)-phenyl]borate anion and the butyltriphenylborate salts of the diphenyliodonium and dimethylphenacylsulfonium cations.[5,8d,13]

III. X-ray Structures of the Pyridinium Borate Salts. To pinpoint the origin of the charge-transfer absorption bands of the highly colored pyridinium tetraalkylborate salts, X-ray crystallography was performed on [**iQ$^+$**,BMe$_4^-$] (**4**), [**iQ$^+$**,BMePh$_3^-$] (**8**), and [**NCP$^+$**,BPh$_4^-$] (**15**). For example, the crystal structure of isoquinolinium tetramethylborate salt **4** (Figures 2 and 3) shows that the tetramethylborate anion is located adjacent to the aromatic plane of the *N*-methylisoquinolinium cation with a pair of methyl groups pointed toward the isoquinolinium plane. The distances of the two methyl groups from the aromatic acceptor plane are in the range of van der Waals distance of 3.93 and 3.43 Å, respectively.[14] [Note that such a contact ion pairing has precedent in the crystal structure of charge-transfer salt formed from tetracarbonylcobaltate and *N*-methylquinolinium cation, except the anion in the latter interacts with the cation through three carbonyl oxygen atoms.[9c]] The tetramethylborate moiety is present as a discrete tetrahedral anion with a slight distortion from ideal T_d symmetry. The corresponding bond angles and lengths for BMe$_4^-$ are listed in Table 2. This interionic separation is in contrast to the structure of LiBMe$_4$, which shows the strong interaction between the methyl group and the lithium cation to weaken the B−C bonds sufficiently to distort the BMe$_4^-$ moiety from ideal
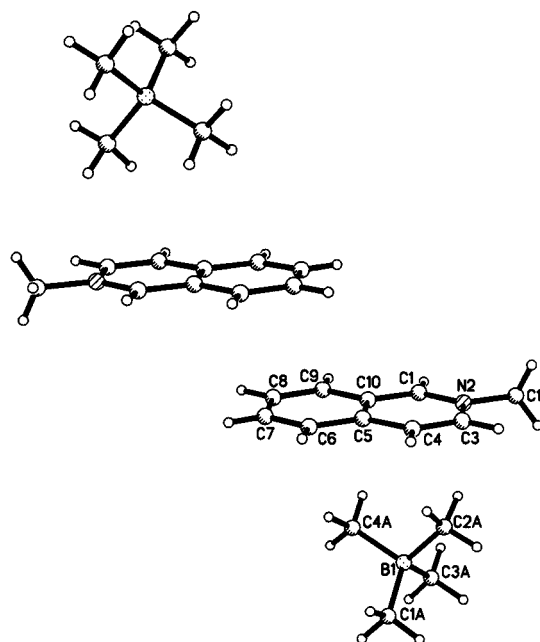

Figure 2. Contact charge-transfer ion pairs from the X-ray crystallography of isoquinolinium tetramethylborate (**4**). The critical interactions are as follows: C2A/iQ$^+$ plane 3.42, C4A/iQ$^+$ plane 3.93, iQ$^+$ plane/iQ$^+$ plane 3.42, C2A/C1 3.54, C2A/N 3.45, and C2A/C3 3.78 Å.
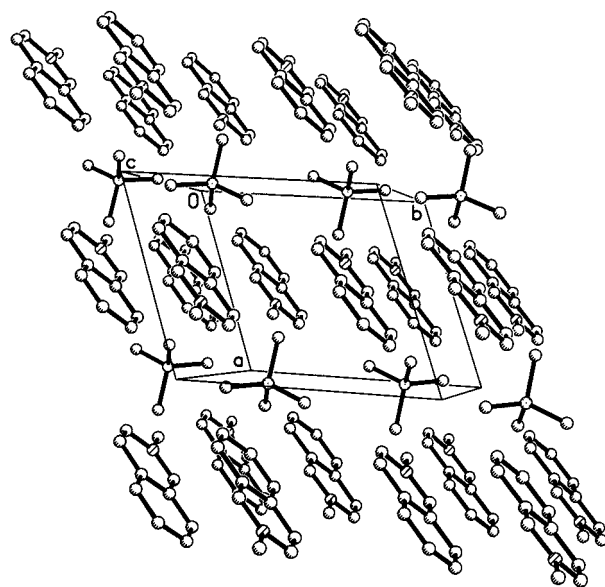

Figure 3. Packing diagram of isoquinolinium tetramethylborate (**4**).

tetrahedral configuration.[15] The isoquinolinium cation is in van der Waals contact ($d = 3.42$ Å with slight $\pi-\pi$ overlap) with another cation.

For [**iQ$^+$**,BMePh$_3^-$], the methyltriphenylborate anion interacts with the isoquinolinium cation through a phenyl group rather than the methyl group, as shown in Figure 4. The packing diagram in Figure 5 shows that the partial overlap of two isoquinolinium cations is consistent with the $\pi-\pi$ interaction at a distance between the two aromatic cation planes of 3.43 Å.[16]

(11) Irreversible anodic peak potentials of BMe$_4^-$, BMePh$_3^-$, and BPh$_4^-$ were 0.575, 0.957, and 0.99 V (SCE), respectively, as measured by cyclic voltmmetry at a scan rate of 100 mV/s in THF containing 0.1 M (*n*-Bu)$_4$N$^+$PF$_6^-$ as supporting electrolyte.

(12) Mulliken, R. S. *J. Am. Chem. Soc.* **1952**, *74*, 811.

(13) (a) Taba, Y.; Yasuike, M.; Usui, Y. *J. Chem. Soc., Chem. Commun.* **1997**, 675. (b) Nagamura, T. *Pure Appl. Chem.* **1996**, *68*, 1449. (c) Nagamura, T.; Sakai, K. *J. Chem. Soc., Chem. Commun.* **1986**, 810.

(14) The van der Waals radius of the methyl group is 2.0 Å, and the half-thickness of the aromatic molecule is taken as 1.70 Å. Pauling L. *The Nature of the Chemical Bonds*, 3nd ed.; Cornell Unversity Press: Ithaca, 1960.

(15) (a) Barr, D.; Snaith, R.; Mulvey, R. E.; Perkins, P. G. *Polyhedron* **1988**, *7*, 2119. (b) Rhine, W. E.; Stucky, G.; Peterson, S. W. *J. Am. Chem. Soc.* **1975**, *97*, 6401.
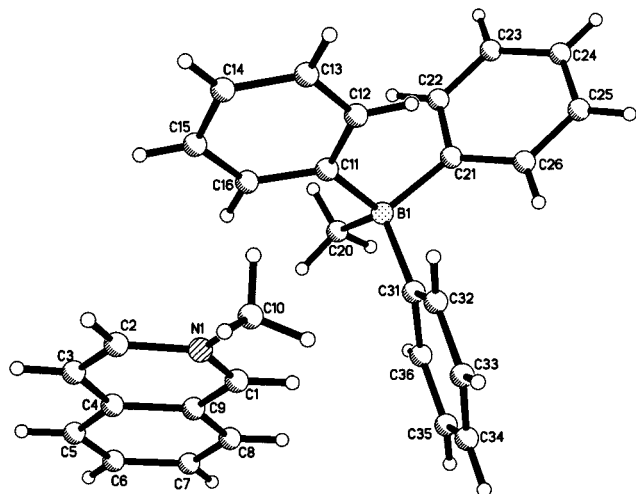
Figure 4. ORTEP diagram of the contact ion pair in isoquinolinium methyltriphenylborate (**8**). The critical interactions are as follows: C15/C2 3.69, C15/N1 3.54, C16/N1 3.42, C16/C1 3.51 Å, and the dihedral angle between the iQ$^+$ plane and the phenyl(1) plane is 11.16°.
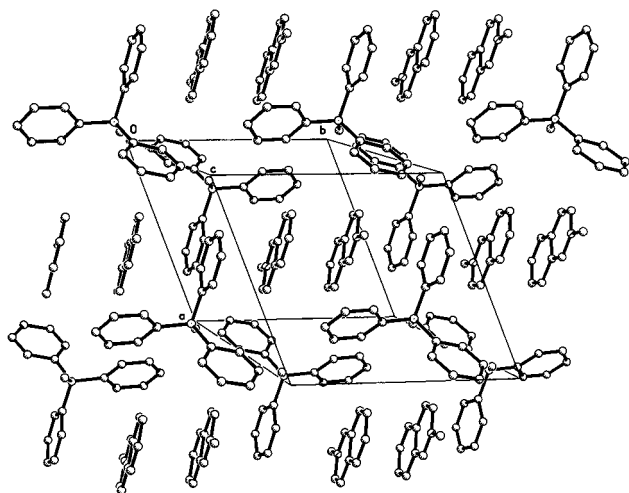

Figure 5. Packing diagram of isoquinolinium methyltriphenylborate (**8**).

Table 2. Bond Distances and Bond Angles for BMe$_4^-$ and BMePh$_3^-$ in the Charge-Transfer Salts with Isoquinolinium Cation

	BMe$_4^-$	BMePh$_3^-$
B–C	1.639(2)	1.653(2) (B-Me)
	1.6408(14)	1.654(2)
	1.6414(14)	1.659(2)
	1.648(2)	1.660(2)
C–B–C	109.40(8)	109.71(9)
	109.76(8)	109.11(9)
	110.76(8)	111.05(9)
	109(31)(8)	111.05(9)
	109.51(10)	108.10(9)
	108.08(9)	107.81(8)

Although the crystallographic disorder of [**NCP**$^+$, BPh$_4^-$] (Figures 6 and 7) precluded a more detailed discussion of the interaction of the anion and the cation,

---

(16) Each of the two isoquinolinium cations was in contact with two phenyl groups from two methyltriphenylborate anions, with one being near the positively charged nitrogen atom and the other being slightly overlapped with the aromatic acceptor ring at the other end (Figure 5). This donor–acceptor orientation is likely to result from the π–π interaction between the phenyl group and the isoquinolinium ring.
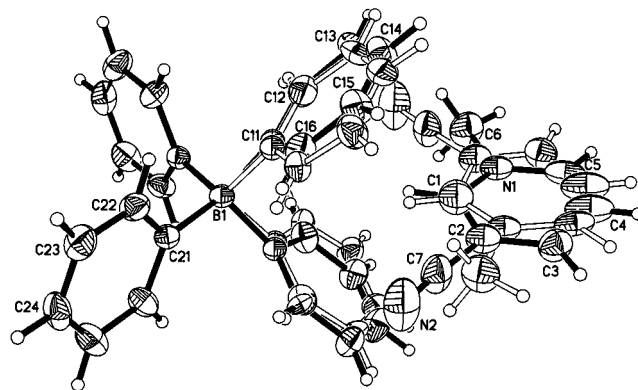

Figure 6. Structure of the penetrated ion pair in 3-cyanopyridinium tetraphenylborate (**15**) showing numbering of atoms. Thermal ellipsoids are drawn with 50% probability.
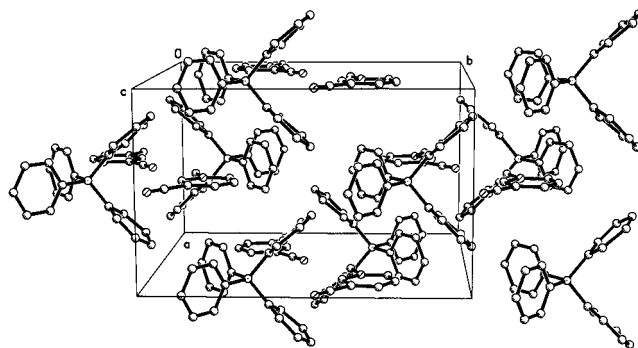

Figure 7. Packing diagram of 3-cyanopyridinium tetraphenylborate (**15**).

it was sufficient to show that the 3-cyanopyridinium cation is located between the two phenyl groups of the tetraphenylborate anion to form a penetrated ion pair.[17] This orientation is preferred for optimum π–π interaction between the phenyl groups and the acceptor ring. Therefore, such X-ray crystallographic analysis established that these charge-transfer salts consist of contact ion pairs with interionic separations that are relevant to the charge-transfer absorption band.[18]

IV. Interionic Methyl Transfer in Pyridinium Borate Salts. The crystalline pyridinium borates reacted upon their dissolution in tetrahydrofuran. For example, the yellow-orange color of [**iQ**$^+$,BMe$_4^-$] in THF solution was discharged within an hour at room temperature. When the solvent was removed from the colorless solution, a 96% yield of 1,2-dihydro-1,2-dimethylisoquinoline was isolated. The byproduct, trimethylborane, was formed in quantitative yield (as assessed by ^{1}H NMR spectroscopy), and it was isolated as the crystalline adduct with ammonia. [See the Experimental Section for a complete description of the reaction.] The reaction was thus identified as the formal transfer of methide (CH$_3^-$) from tetramethylborate to the isoquinolinium cation, i.e.,

---

(17) (a) Murphy, S.; Yang, X. Q.; Schuster, G. B. *J. Org. Chem.* **1995**, *60*, 2411. (b) Koska, N. A.; Wilson, S. R.; Schuster, G. B. *J. Am. Chem. Soc.* **1993**, *115*, 11628. (c) Yang, X. Q.; Zactsev, A.; Sauerwein, B.; Murphy, S.; Schuster, G. B. *J. Am. Chem. Soc.* **1992**, *114*, 793.

(18) (a) Bockman, T. M.; Kochi, J. K. In *Photosensitization and Photocatalysis Using Inorganic and Organometallic Compounds*; Kalyanasundaram, K., Gratzel, M., Eds.; Kluwer Acadamic Publishers: The Netherlands, 1993; p 407. (b) Kochi, J. K.; Bockman, T. M. *Adv. Organomet. Chem.* **1991**, *33*, 52.

Table 3. Thermal Methyl Transfer of the Charge-Transfer Salts

Entry	CT Salt	Reaction Conditions[a]	Product and Yield(%)[b]
1	isoquinolinium + BMe₄⁻	THF-d₈/1h	(100)[c] + BMe₃ (100)[c]
2	isoquinolinium + BMe₄⁻	1h	(96) + BMe₃ (68)[d]
3	quinolinium BMe₄⁻	1h	(100)
4	quinolinium BMe₄⁻	THF-d₈/1h	(89)[c] + BMe₃ (89)[c]
5	phenanthridinium BMe₄⁻	THF-d₈/1h	(100)[c] + BMe₃ (100)[c]
6	phenanthridinium BMe₄⁻	CD₃CN/1h	(100)[c]
7	acridinium + LiBMe₄ OTf	1 h	(79) + (20)
8	3-cyano-pyridinium + LiBMe₄ OTf	1 h	(68) + (29) + (trace)[c]

[a] In THF at room temperature, unless indicated otherwise. [b] Isolated yield at 100% conversion. [c] Yield determined by ¹H NMR analysis. [d] Isolated as the ammonia adduct.

$$\text{isoquinolinium}^+ BMe_4^- \longrightarrow \text{dihydroisoquinoline} + BMe_3 \quad (3)$$
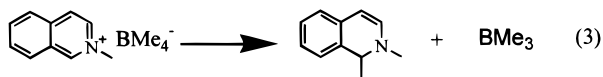
An analogous transfer of methide occurred immediately upon the dissolution of the BMe₄⁻ salt of *N*-methylphenanthridinium in THF, and 5,6-dihydro-5,6-dimethylphenanthridine was isolated in 89% yield. The same reaction occurred more slowly in the polar solvent, acetonitrile, but the reaction was nonetheless complete within an hour (Table 3).
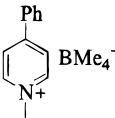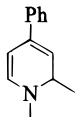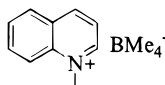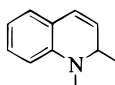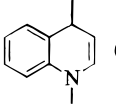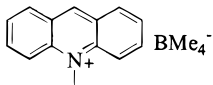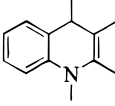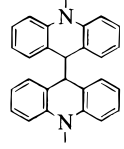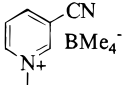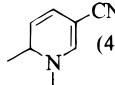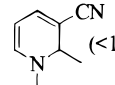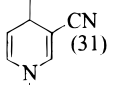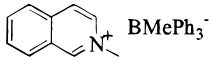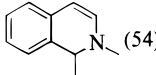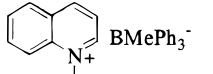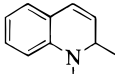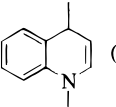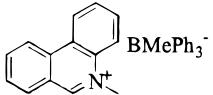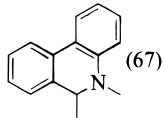
For the most reactive tetramethylborate salts of 3-cyano-*N*-methylpyridinium and *N*-methylacridinium, the rapidity of the methide transfer precluded isolation of the charge-transfer salt. In these cases, the reactive salt was generated in situ by addition of the lithium salt of BMe₄⁻ to a suspension of the pyridinium salt. For example, when lithium tetramethylborate was mixed with 3-cyano-*N*-methylpyridinium triflate in THF, methyl transfer led to a mixture of 3-cyano-1,6-dihydro-1,6-dimethylpyridine and 3-cyano-1,2-dihydro-

1,2-dimethylpyridine in 68% and 29% yields, respectively. In the case of *N*-methylacridinium, the usually high yield of the product of methyl transfer (>90%) was slightly reduced (entry 9 in Table 3). The difference was accounted for by the formation of *N,N*-dimethyl-10,10′-biacridanyl (in 20% yield), as the product of reductive dimerization. It is noteworthy that the alkylation of pyridinium cations under these conditions is much more efficient than previously reported procedures using nucleophiles such as alkyllithium, Grignard, and cuprate reagents, in which isomeric mixtures were usually obtained in low yields.[19]

V. Photoinduced Methyl Transfer. The borate salts which did not react spontaneously at room temperature could be induced to react by the deliberate irradiation of their charge-transfer absorption bands.[20]

(19) (a) Stout, D. M.; Meyers, A. I. *Chem. Rev.* **1982**, *82*, 223. (b) Bradley, W.; Jeffrey, S. *J. Chem. Soc.* **1954**, 2770. (c) Francis, R.; Davis, W.; Wisener, J. *J. Org. Chem.* **1974**, *39*, 59. (d) Piers, E.; Sauey, M. *Can. J. Chem.* **1974**, *52*, 3563.

Table 4. Photoinduced Methyl Transfer of the Charge-Transfer Salts

Entry	CT Salt	Reaction Conditions[a]	Product and Yield(%)[b]
1	Ph–pyridinium, BMe$_4^-$	8h	Ph (75)
2	quinolinium, BMe$_4^-$	-78°C/1h	(79) + (19)
3	acridinium, BMe$_4^-$	-78°C/1 h	(10) + (85)
4	CN-pyridinium, BMe$_4^-$	-78°C/1 h	(48) + (<1) + (31)
5	isoquinolinium, BMePh$_3^-$	3h	(54)
6	quinolinium, BMePh$_3^-$	3h	(45) + (10)
7	phenanthridinium, BMePh$_3^-$	1h	(67)

[a] Irradiated at CT band in THF at room temperature unless indicated otherwise. [b] Isolated yield at 100% conversion. The isomer ratio of the mixture determined by ^{1}H NMR analysis.

Although the tetramethylborate salt of 4-phenylpyridinium did not react after 24 h in the dark, upon irradiation at λ_{exc} > 370 nm, the yellow solution bleached, and workup by preparative TLC yielded the product of methide transfer, 1,2-dihydro-1,2-dimethyl-4-phenylpyridine in 75% yield. In the case of those borate salts that reacted at room temperature, photolysis was carried out at −78 °C to obviate any competition from the thermal reaction (at this low temperature). It is noteworthy that the photoinduced transfer of CH_3^- conformed to the same stoichiometry as the thermal reaction (Table 4), i.e.,

$$[\mathbf{Py}^+, \mathbf{BMe}_4^-] \xrightarrow{h\nu_{CT}} \mathbf{Py}\text{-Me} + \mathbf{BMe}_3 \qquad (4)$$

The exception was the photoreaction of *N*-methylacridinium with tetramethylborate, which yielded the dimeric *N,N*-dimethyl-10,10′-biacridanyl as the major product.

Photoactivation of the thermally stable methyltriphenylborates could also be carried out as summarized in Table 4. In each case, the product of methide transfer

was obtained, and no Ph⁻ transfer could be detected by either ^{1}H NMR and/or GC−MS analysis.[21]

VI. Comparison of Thermal and Photochemical Reactions. The pyridinium cations, 3-cyano-*N*-methylpyridinium and *N*-methylquinolinium, were used to compare the isomer distribution of the methylated pyridines in the thermal and photochemical reactions. As shown in Table 5, the thermal reaction of 3-cyano-*N*-methylpyridinium with tetramethylborate yielded 3-cyano-1,6-dihydro-1,6-dimethylpyridine and 3-cyano-1,2-dihydro-1,2-dimethylpyridine as the major products, whereas the photoinduced methyl transfer led to 3-cyano-1,6-dihydro-1,6-dimethylpyridine and 3-cyano-1,4-dihydro-1,4-dimethylpyridine in 48% and 31% yields, respectively. In the case of *N*-methylquinolinium, both thermal and photoinduced methyl transfer preferentially afforded 1,2-dihydro-1,2-dimethylquinoline, although the yield of the isomeric 1,4-dihydro-1,4-dimethylquinoline in the photoreaction (19%) was somewhat

(20) Irradiation was carried out with a cutoff filter (>370 or 410 nm), so that only the charge-transfer band of the pyridinium borates was irradiated.

(21) Photoinduced alkylations of other acceptors by alkyltriphenylborates have appeared in the literature.[22] In all of these cases, however, the local absorption band of the acceptors was irradiated, so that the excited acceptors were quenched by borates via electron-transfer processes leading to alkyl transfer. For example, Schuster showed that irradiation of the acetonitrile solutions of dicyanoarenes with methyl- or benzyltriphenylborates afforded alkylcyanoarenes.[22a,b] Matsuoka and Lund reported the butyl transfer from butyltriphenylborate to the excited cyanine cation[22c] or anthracene,[22d] respectively.

Table 5. Isomer Distribution of Methyl-Transfer Adducts

CT Salt	Reaction Conditions	Isomer Distribution		
(structure)	r.t.	68	29	<1
	-78 °C to r.t.	68	30	<1
	-78 °C/hv	48	<1	31
(structure)	r.t.	100		0
	0 °C	95		<5
	-78 °C/hv	79		19

Table 6. Competitive Alkyl Transfer of Mixed Organoborate (BR_3R') to Isoquinolinium Cation

R	R′	reaction conditions	A−R	A−R′
Me	n-Bu	r.t.	68	17
Me	n-Bu	−78 °C to r.t.	39	58
n-Bu	s-Bu	−78 °C to r.t.	15	75
Me	n-Bu	hv/−78 °C	28	55

higher than that in the thermal reaction (<1%). Despite the slight difference, predominant alkylation occurred at the carbon atoms bonded to the positively charged nitrogen atom both in the thermal reaction and the photoreaction. This suggested that the orientation of the donor and the acceptor in the ground state of charge-transfer complexes may play an important product-determining role.[23]

VII. Competitive Alkyl Transfer from Mixed Alkylborates. To gain some insight into the mechanism of methyl transfer, *n*-butyltrimethylborate and *sec*-butyltri(*n*-butyl)borate were prepared, and the relative transferability of methyl, *n*-butyl, and *sec*-butyl groups were examined using *N*-methylisoquinolinium cation as the electrophile. As shown in Table 6, the alkyl transfer from alkylborate to isoquinolinium cation was highly dependent on the structure of the alkyl group, the relative rates of alkyl transfer increasing in the order methyl < *n*-butyl < *sec*-butyl = 1:4.5:67.5 (after normalization for the statistical factors). In the photoinduced alkyl transfer, *n*-butyl was transferred about 6 times faster than the methyl group. These results run counter to the expectations based on the pattern observed in the conventional nucleophilic alkyl transfer reactions of the same borates. [For example, Negishi et al. reported that in mixed tetraalkylborates containing both primary and secondary alkyl groups the primary

Table 7. Solid-State Reaction of the Charge-Transfer Salts

Entry	CT Salt	Reaction Conditions[a]	Product & yield (%)[b]
1	(structure) BMe_4^-	r.t./18h	(structure) (99) + BMe_3 (76)[c]
5	(structure) BMe_4^-	5h	(structure) (71)
5	(structure) $BMePh_3^-$	48h	d,e
6	(structure) $BMePh_3^-$	48h	d,e
7	(structure) $BMePh_3^-$	26h	(structure) (20)[e]

[a] Irradiated at CT band at 0 °C, except entry 1, which was a thermal reaction. [b] Isolated yield. [c] Isolated as ammonia adduct. [d] No alkylated product was detected. [e] Determined by ^{1}H NMR analysis.

alkyl group was transferred to acyl halides exclusively (independent of statistical factors).[3,4]]

VIII. Solid-State Reaction of the Charge-Transfer Salts. Efficient methyl transfer could be effected in the solid state. When the crystalline *N*-methylphenanthridinium salt of tetramethylborate was stored at room temperature, the orange crystal visibly darkened overnight to form a red amorphous residue, and the mixture liberated a flammable gas. The residue was purified and characterized as 9,10-dihydro-9,10-dimethylphenanthridine, and the gas was identified as trimethylborane (as an adduct with ammonia, see Experimental Section). For [iQ^+,BMe_4^-], which did not react spontaneously in the solid state, the methyl transfer could be induced by irradiating the charge-transfer absorption band of the crystalline salt to afford 1,2-dihydro-1,2-dimethylisoquinoline in 71% yield. In the cases of methyltriphenylborate, methyl transfer in the solid state was inefficient (Table 7), and irradiation of charge-transfer band of the *N*-methylphenanthridinium methyltriphenylborate produced 9,10-dihydro-9,10-dimethylphenanthridine in only 20% yield. No methyl transfer product was obtained for either [iQ^+,$BMePh_3^-$] or [Q^+,$BMePh_3^-$]. Such an inefficiency was consistent with the X-ray structure of [iQ^+,$BMePh_3^-$], which revealed that *N*-methylisoquinolinium cation is located beside the phenyl group (not at the methyl group) of the borate anion in the crystal lattice (Figure 5).

Discussion

Electron-Transfer Mechanism for Photoinduced Nucleophilic Addition. Irradiation of the charge-transfer band of donor/acceptor complexes directly effects electron transfer from the donor to the acceptor.[24] This charge-transfer process follows from Mulliken theory and has been verified by laser-spectroscopic studies.[12,24] In particular, pyridinium salts of donor anions such as iodide and various carbonylmetalates

(22) (a) Lan, J. Y.; Schuster, G. B. *Tetrahedron Lett.* **1986**, *27*, 4261. (b) Lan, J. Y.; Schuster, G. B. *J. Am. Chem. Soc.* **1985**, *107*, 6710. (c) Matsuoka, M.; Hikida, T.; Murobushi, K.; Hosoda, Y. *J. Chem. Soc., Chem. Commun.* **1993**, 299. (d) Lund, T. *Acta Chem. Scand.* **1996**, *50*, 64.

(23) Kosower, E. M. *Prog. Phys. Org. Chem.* **1965**, *3*, 81.

(24) Kochi, J. K. *Adv. Phys. Org. Chem.* **1994**, *29*, 185.

yield pyridinyl radicals and the oxidized anion both in solution and in the solid state.[9c] For the charge-transfer salts of the pyridinium borates in Chart 1, such a process leads to the geminate radical pair composed of the pyridinyl radical and the tetraalkylboranyl radical (eq 2). Since the methyl transfer from tetramethylborate to the pyridinium cation is the consequence of charge-transfer photostimulation, it follows that this typical nucleophilic process must also proceed by an initial electron transfer from tetramethylborate (acting as an electron donor) to the pyridinium acceptor. Previous attempts to apply the charge-transfer formulation to nucleophilic reactions of CT ion pairs have been unsuccessful largely owing to the efficiency of the back electron transfer (k_{BET}) to restore the original ion pair. For example, CT excitation of the charge-transfer salt of tetrakis[3,5-bis(trifluoromethyl)phenyl]borate anion with 4,4′-bipyridinium cation gives rise to reversible electron transfer, and no photochemistry has been reported.[13b,c] Since the back electron transfer generally occurs a few picoseconds after photoactivation, the methyl transfer must occur very rapidly in order to compete. It should also be emphasized that the products of pyridinyl/pyridinyl coupling (to produce the dihydro dimers, **Py−Py**) are not among the products of the photoreaction (except in the case of the *N*-methylacridinium ion). These dimers are readily formed whenever pyridinium cations are reduced by chemical and electrochemical means,[25] and their absence from the mixture of products indicates that methyl transfer must occur prior to the diffusive separation of the [**Py•**,BR₄•] radical pair in eq 5.

$$[\mathbf{Py^•},BR_4^•] \xrightarrow{fast} [\mathbf{Py}\text{-}R,BR_3] \qquad (5)$$
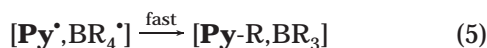
The actual (formal) transfer of the methyl radical to give the products thus occurs within the solvent cage, and free pyridinyl radicals are not involved.

We now inquire as to how the methyl transfer can outrun the back electron transfer. Spin-trapping studies have shown that tetraalkylborate anions (R₄B⁻) readily yield alkyl radicals (R•) upon anodic (one-electron) oxidation,[26] i.e.,

$$BR_4^- \xrightarrow{-e} BR_4^• \xrightarrow{k_{CB}} BR_3 + R^• \qquad (6)$$
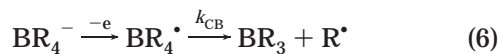
and time-resolved experiments have shown that the scission of the C−B bond occurs on the picosecond or subpicosecond time scale.[27] As such, we suggest that fragmentation (k_f) is the crucial step in the methyl transfer reaction and that the products are formed in the subsequent coupling of the methyl and pyridinyl radicals, as formulated in Scheme 1

Implications to the Mechanism of Thermal Nucleophilic Addition. The thermal reactions of the various pyridinium tetramethylborates yield the same products (i.e., trimethylborane and the methylated

Scheme 1

$$[\mathbf{Py^+},BR_4^-] \xrightarrow{h\nu_{CT}} [\mathbf{Py^•},BR_4^•] \qquad (2)$$

$$[\mathbf{Py^•},BR_4^•] \xrightarrow{k_f} [\mathbf{Py^•},Me^•,BMe_3] \qquad (7)$$

$$[\mathbf{Py^•},Me^•,BMe_3] \xrightarrow{k_{RR}} \mathbf{Py}\text{-}Me + BMe_3 \qquad (8)$$

dihydropyridine) as those obtained by the photochemical CT activation. In other words, methyl transfer can be effected either by charge-transfer photolysis or by thermal activation. For example, the photolysis of 3-cyano-*N*-methylpyridinium tetramethylborate at −78 °C yields the same mixture of dimethyldihydrocyanopyridines as that obtained simply by warming the solution to room temperature in the dark. The virtual identity of the products from the two modes of reaction raises the question of whether the thermal reaction also proceeds by the mechanism in Scheme 1. To probe this question, we examined in more detail the product distributions from the thermal and photochemical reactions. We note that the product of the reaction is highly dependent on the structure of the transferred alkyl group, the relative transfer rate increasing in the order methyl < *n*-butyl < *sec*-butyl = 1:4.5:67.5. These results run counter to the expectation from a conventional nucleophilic process where the less hindered group is transferred preferentially.[28] Since the observed order reflects the decreasing strength of the B−C bond,[7,8] the cleavage of this bond is a critical step. We thus conclude that the thermal reaction proceeds via essentially the same intermediates as those in the photoinduced reaction, both following the sequence of steps shown in Scheme 1.

Charge-Transfer Ion Pairs as Critical Intermediates in Nucleophilic Addition. The interionic charge-transfer interaction between tetraalkylborates, such as tetramethylborate, methyltriphenylborate, and tetraphenylborate, and a series of pyridinium cations has been characterized by their CT absorption bands in solution and in the solid state. The colors of these salts are associated with the CT absorption not present in either the donor anions (as tetrabutylammonium salt) or the acceptor cations (as triflate salt). As a consequence of the charge-transfer nature of these absorption bands, the CT bands in both the solid state and in solution are consistently red-shifted as the acceptor strength (E_{red}) of the cation increases in the order **mC⁺** < **mL⁺** < **PP⁺** < **iQ⁺**. Furthermore, the same red shift applies to the charge-transfer transitions of the corresponding methyltriphenylborate and tetraphenylborate salts. The progressive bathochromic shift of the charge-transfer absorption bands (λ_{CT}) in the solid state with the decreasing reduction potentials of the cations is illustrated in Figure 8. The linear relationship follows from the Mulliken theory of charge-transfer,[12] in which the CT energy ($h\nu_{CT}$) for a given electron donor can be expressed by

$$h\nu_{CT} = aE_{red}(A) + \text{constant} \qquad (9)$$

where $E_{red}(A)$ is the reduction potential of the pyridinium acceptor.[12]

(25) (a) Schwarz, M.; Hermolin, J.; Kirowa-Eisner, E. *J. Electroanal. Chem.* **1987**, *220*, 139. (b) Oturan, M. A.; Dostert, P.; Benedetti, M. S. *J. Electroanal. Chem.* **1988**, *242*, 171. (c) Carelli, I.; Cardinali, M. E.; Casini, A.; Arnone, A. *J. Org. Chem.* **1976**, *41*, 3967.
(26) Bancroft, E. E.; Blount, H. N. *J. Am. Chem. Soc.* **1979**, *101*, 3692.
(27) The lower limit for the rate of B−C bond cleavage in boranyl radicals of the type R−BPh₃ (R = alkyl or benzyl) is 10¹¹ S⁻¹; see ref 7.
(28) March, J. *Advanced Organic Chemistry*, 4th ed.; John Wiley & Sons: New York, 1992; p 186.
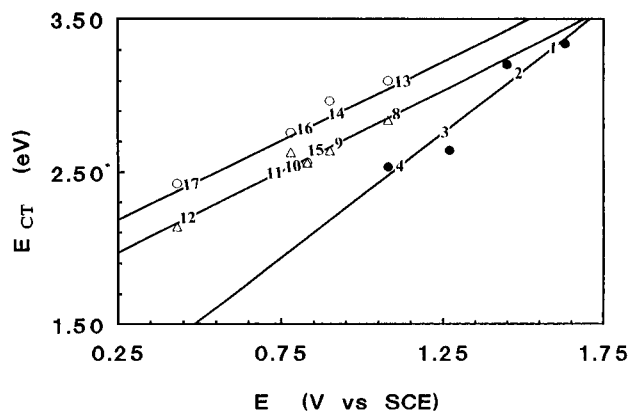
Figure 8. Mulliken correlation of the solid-state CT absorption bands of BMe_4^- (●), $BMePh_3^-$ (△) and BPh_4^- (○) salts versus the reduction potentials of various pyridinium cations as identified in Table 1.
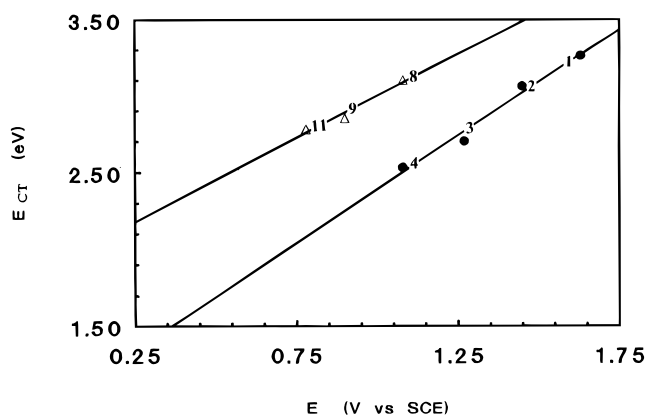

Figure 9. Mulliken correlation of the CT absorption bands in THF solutions of BMe_4^- (●) and $BMePh_3^-$ (△) salts versus the reduction potentials of various pyridinium cations.

A similar cation- and anion-dependent shift (Figure 9) is observed for the charge-transfer salts dissolved in nonpolar solvents such as THF. Most importantly, the various CT bands and their associated colors vanish upon dissolution of these salts in acetonitrile, in which ion-pair dissociation leads to the solvent-separated ion pair. The contact ion pair is the critical species for the formation of charge-transfer salts.[18] [It should be pointed out that the slope of the Mulliken plot for tetramethylborate is greater than those of methyltriphenylborate and tetraphenylborate, as shown in Figure 8. This deviation may suggest that the precise mode of the charge-transfer interaction in tetramethylborate salts is different from that in the other two borate salts.]

Contact ion pairing pertinent to charge-transfer interaction is also identified in the solid state by X-ray crystallography. The isolation of the colored charge-transfer salts and X-ray crystal structure analysis show the close contacts between anion and cation that are critical for effective charge-transfer interaction. Indeed, we find in the X-ray structure of $[iQ^+, BMe_4^-]$ that the two methyl groups of the tetramethylborate anion are in van der Waals contact with the acceptor cation for the optimal overlap with the π-LUMO of the isoquinolinium cation (Figure 2).[29] Since the HOMO of the tetramethylborate can be reasonably considered to have σ character, the interionic contact between the tetra-

methylborate anion and the pyridinium cations can be considered as the $\sigma-\pi$ interaction. In contrast, methyltriphenylborate and tetraphenylborate anions interact with the cations via slight overlap between the π orbital of the phenyl group of the borate anion and the π-LUMO of the aromatic acceptor cations (Figures 4 and 6). This diversity in the interaction modes may also be reflected in the difference in the slopes of the Mulliken plots.

Charge-transfer ion pairs are critical intermediates in methyl transfer to pyridinium cations, since both their thermal and photochemical charge-transfer excitations lead to efficient alkylation of the pyridinium acceptors. In addition, the orientation of the donor and the acceptor in the ground state of charge-transfer complexes plays an important role in determining the product structure, both in the thermal reaction and in the photoreaction.[23] In the ground state of the charge-transfer complexes, the specific interaction between the negative center of the borate anion and the positively charged nitrogen of the pyridinium cation brings the methyl group close to the carbon atoms bonded to the positively charged nitrogen atom. For example, in $[iQ^+, BMe_4^-]$ (Figure 2) the distances from C2A to C1, N, and C3 are 3.54, 3.45, and 3.78 Å, respectively. When multiple positions on pyridinium cations are available for alkylation, preferential alkylation occurs at the carbon atoms adjacent to the nitrogen atom (in both the thermal and photochemical reactions). For example, Table 5 shows that in the thermal and photochemical reactions of 3-cyano-N-methylpyridinium with tetramethylborate the major product is 3-cyano-1,6-dihydro-1,6-dimethylpyridine. In the case of N-methylquinolinium, 1,2-dihydro-1,2-dimethylquinoline is the major product, although the yield of the isomeric 1,4-dihydro-1,4-dimethylquinoline is higher in the photoreaction than in the thermal reaction.

The importance of the orientation of the donor and the acceptor in the charge-transfer complexes is even more critical in the solid state. Thus irradiation of the charge-transfer absorption bands of the tetramethylborate salts of pyridinium cations in the solid state leads to efficient methyl transfer to afford methylated dihydropyridines in high yields, whereas methyl transfer is not efficient when the methyltriphenylborate salts are irradiated under the same conditions. This is understandable if we consider the topological requirements of the solid-state reaction[30] in which the exact orientation of methyltriphenylborate anion relative to the pyridinium cation is apparent from crystal packing in the unit cell. As shown in Figures 4 and 5, a phenyl group of the methyltriphenylborate anion interacts with the isoquinolinium cation via weak $\pi-\pi$ interaction (and the methyl group is not close to the cation). CT excitation in the solid state occurs via electron transfer from the anion to the cation to generate the pyridinyl radical and the methyltriphenylboranyl radical pair in the crystal lattice. Since the B–Me bond is much weaker than the B–Ph bond, methyl cleavage is preferred.[7,8] However, any subsequent combination of methyl radical

(29) The LUMO of pyridinium cations is a π^* orbital centered on the aromatic ring. (a) Grossi, L.; Minisci, F.; Pedulli, G. F. *J. Chem. Soc., Perkin Trans. 2* **1977**, 943. (b) Itoh, M.; Nakagura, S. *J. Am. Chem. Soc.* **1967**, *89*, 3959.
(30) Schmidt, G. M. J. *Pure Appl. Chem.* **1971**, *27*, 647.

with the pyridinyl radical is disfavored, since they are constrained by the crystal lattice and not in close proximity.

Conclusion

The transfer of the methyl from tetramethylborate to pyridinium cations is effected by charge-transfer photolysis of the [Py^+,BMe_4^-] ion pair, which establishes the nucleophilic addition to the pyridinium ring to proceed via an initial electron transfer from the borate donor to the pyridinium acceptor. The final products of methyl transfer are formed in a subsequent radical/radical coupling step that occurs within the solvent cage. The thermal reactions of the charge-transfer salts yield the same methyl transfer products, and thus they are likely to proceed via an analogous thermally induced electron transfer. Critical to both the thermal and photoinduced processes is the interionic charge-transfer interaction between the borate donor and the pyridinium acceptor that is structurally identified by X-ray crystallography of the isolated charge-transfer salts.

Experimental Section

Materials. Trimethylborane,[31] LiBMe$_4$,[31] LiBMePh$_3$,[32] and various pyridinium salts[33] in Chart 1 were prepared according to the literature procedures. Methyllithium, tri(*n*-butyl)borane, triphenylborane, and sodium tetraphenylborate were from Aldrich and used as received. All manipulations were carried out under an atmosphere of argon using standard Schlenk techniques or in a drybox. Solvents (tetrahydrofuran, diethyl ether, and benzene) were freshly distilled under argon from sodium/benzophenone. Acetonitrile was refluxed over 0.1% KMnO$_4$ for 1 h and then redistilled serially from P$_2$O$_5$ and CaH$_2$. Distilled water was deoxygenated by purging with argon prior to use. NH$_3$ was dried with sodium and distilled before use. UV–visible spectra of the change-transfer salts in THF solution (0.005 M) and the solid state (0.1 mmol/g silica gel) were measured on a Hewlett-Packard 8450A diode-array spectrometer and a Varian Cary 5G UV–vis–NIR spectrometer, respectively. ^{1}H and ^{13}C NMR spectra were recorded on a General Electric QE-300 spectrometer.

General Procedure for the Preparation of Charge-Transfer Salts. *N*-Methylisoquinolinium Tetramethylborate (4). An aqueous solution of LiBMe$_4$ (78 mg, 1.0 mmol) was added into an aqueous solution of *N*-methylisoquinolinium triflate (293 mg, 1.0 mmol) slowly. A yellow solid precipitated immediately. The yellow precipitate was filtered off and washed with water. Recrystalization by diffusion of diethyl ether into the acetonitrile solution at −30 °C afforded yellow needle crystals, 200 mg, 93% yield. ^{1}H NMR (CD$_3$CN): δ (ppm) −0.690 (q, $^2J_{B-H}$ = 3.9 Hz, 12H, BMe$_4$), 4.419 (s, 3H, N−CH$_3$), 7.90−8.50 (m, 7H, ArH). ^{13}C NMR (CD$_3$CN): δ (ppm) 17.866 (q, $^2J_{B-C}$ = 157 Hz, BMe$_4$), 48.186 (N−CH$_3$), 126.149, 127.328, 127.572, 129.962, 131.580, 135.277, 137.151, 150.002 (aromatic carbons).

***N*-Methyl-2,4,6-collidinium tetramethylborate (1):** white solid, 97% yield; ^{1}H NMR (CD$_3$CN) δ (ppm) −0.701 (q, $^2J_{B-H}$ = 3.9 Hz, 12H, BMe$_4$), 2.489 (s, 3H, CH$_3$), 2.678 (s, 6H, CH$_3$), 3.900 (s, 3H, N−CH$_3$), 7.522 (s, 2H, ArH); ^{13}C NMR (CD$_3$CN) δ (ppm) 17.792 (q, $^2J_{B-C}$ = 157 Hz, BMe$_4$), 20.515 (4-CH$_3$),

20.895 (2,6-CH$_3$), 39.509 (N−CH$_3$), 127.707, 154.846, 157.761 (aromatic carbons). Elemental Anal. Calcd for C$_{13}$H$_{26}$BN (207.17): C, 75.37; H, 12.65; N, 6.76. Found: C, 75.32; H, 12.36; N, 6.80.

***N*-Methyl-2,6-lutidinium tetramethylborate (2):** white solid, 95% yield; ^{1}H NMR(CD$_3$CN) δ (ppm) −0.700 (q, $^2J_{B-H}$ = 3.9 Hz, 12H, BMe$_4$), 2.745 (s, 6H, CH$_3$), 3.970 (s, 3H, N−CH$_3$), 7.697 (d, J = 7.8 Hz, 2H, ArH), 8.178 (t, J = 7.8 Hz, 1H, ArH); ^{13}C NMR(CD$_3$CN) δ (ppm) 17.820 (q, $^2J_{B-C}$ = 157 Hz, BMe$_4$), 21.284 (2,6-CH$_3$), 40.321 (N−CH$_3$), 127.247, 144.169, 156.136 (aromatic carbons). Elemental Anal. Calcd for C$_{12}$H$_{24}$BN (193.15): C, 74.62; H, 12.52; N, 7.25. Found: C, 74.34; H, 12.38; N, 7.40.

***N*-Methyl-4-phenylpyridinium tetramethylborate (3):** pale yellow solid, 93% yield; ^{1}H NMR(CD$_3$CN) δ (ppm) −0.681 (q, $^2J_{B-H}$ = 3.9 Hz, 12H, BMe$_4$), 4.282 (s, 3H, N−CH$_3$), 7.656 (m, 3H), 7.920(dd, J = 6.3 and 2.1 Hz, 2H), 8.238(d, J = 6.3 Hz, 2H), 8.614(d, J = 6.3 Hz, 2H); ^{13}C NMR(CD$_3$CN) δ (ppm) 17.831 (q, $^2J_{B-C}$ = 157 Hz, BMe$_4$), 47.498 (N−CH$_3$), 124.824, 128.028, 129.767, 132.226, 145.169 (aromatic carbons). Elemental Anal. Calcd for C$_{16}$H$_{24}$BN (241.19): C, 79.68, H, 10.03; N, 5.80. Found: C, 75.45, H, 9.52; N, 5.49.

***N*-Methyl-4-methylquinolinium tetramethylborate (5):** yellow solid, 98% yield; ^{1}H NMR (CD$_3$CN) δ (ppm) −0.694 (q, $^2J_{B-H}$ = 3.9 Hz, 12H, BMe$_4$), 3.002 (s, 3H, CH$_3$), 4.495 (s, 3H, N−CH$_3$), 7.846 (d, J = 5.7 Hz, 1H, ArH), 8.029 (t, J = 7.5 Hz, 1H, ArH), 8.227(t, J = 8.4 Hz, 1H, ArH), 8.323(d, J = 8.4 Hz, 1H, ArH), 8.470 (d, J = 8.4 Hz, 1H, ArH), 8.877(d, J = 5.7 Hz, 1H, ArH); ^{13}C NMR (CD$_3$CN) δ (ppm) 17.781 (q, $^2J_{B-C}$ = 157 Hz, BMe$_4$), 19.408 (4-CH$_3$), 45.126 (N−CH$_3$), 118.899, 122.360, 126.812, 129.691, 135.203 (aromatic carbons).

***N*-Methylquinolinium tetramethylborate (6):** yellow solid, 93% yield; ^{1}H NMR (CD$_3$CN) δ (ppm) −0.693 (q, $^2J_{B-H}$ = 3.9 Hz, 12H, BMe$_4$), 4.561 (s, 3H, N−CH$_3$), 7.95−8.08 (m, 2H, ArH), 8.22−8.30 (m, 1H, ArH), 8.32−8.42 (m, 2H, ArH), 9.03−9.15 (m, 2H, ArH); ^{13}C NMR(CD$_3$CN) δ (ppm) 17.774 (q, $^2J_{B-C}$ = 157 Hz, BMe$_4$), 45.547 (N−CH$_3$), 118.573, 121.726, 130.250, 130.511, 135.913, 147.570 (aromatic carbons).

***N*-Methylphenanthridinium tetramethylborate (7):** orange solid, 96% yield; ^{1}H NMR (CD$_3$CN) δ (ppm) −0.683 (q, $^2J_{B-H}$ = 3.9 Hz, 12H, BMe$_4$), 4.579 (s, 3H, N−CH$_3$), 8.104 (m, 3H, ArH), 8.349 (m, 2H, ArH), 8.431 (m, 1H, ArH), 8.947 (m, 2H, ArH), 9.657 (s, 1H, 10-CH).

***N*-Methylisoquinolinium methyltriphenylborate (8):** very pale yellow solid, 94% yield; ^{1}H NMR (CD$_3$CN) δ (ppm) 0.214 (q, $^2J_{B-H}$ = 3.9 Hz, 3H, B−CH$_3$), 4.241(s, 3H, N−CH$_3$), 6.808 (t, J = 7.2 Hz, 3H, Ph), 6.967 (t, J = 7.2 Hz, 6H, Ph), 7.233 (br, 6H, Ph), 8.000 (m, 1H), 8.192 (m, 3H), 8.274 (m, 2H), 9.192 (m, 1H); ^{13}C NMR (CD$_3$CN) δ (ppm) 12.644 (q, $^2J_{B-C}$ = 165 Hz, B−CH$_3$), 48.048 (N−CH$_3$), 121.486, 125.573, 126.071, 127.277, 129.947, 131.511, 134.185, 135.228, 137.103, 149.954, 167.097 (q, $^2J_{B-C}$ = 195 Hz) (aromatic carbons). Elemental Anal. Calcd for C$_{29}$H$_{28}$BN (401.36): C, 86.78; H, 7.03; N, 3.49. Found: C, 86.91; H, 7.09; N, 3.48.

***N*-Methylquinolinium methyltriphenylborate (9):** pale yellow solid, 95% yield; ^{1}H NMR (CD$_3$CN) δ (ppm) 0.213 (q, $^2J_{B-H}$ = 3.9 Hz, 3H, B−CH$_3$), 4.434 (s, 3H, N−CH$_3$), 6.806 (t, J = 7.2 Hz, 3H, Ph), 6.965 (t, J = 7.2 Hz, 6H, Ph), 7.229 (br, 6H, Ph), 7.884 (t, J = 5.7 Hz, 1H), 8.007 (t, J = 8.4 Hz, 1H), 8.2−8.4 (m, 3H), 8.830 (d, J = 8.4 Hz, 1H), 9.000 (d, J = 5.7 Hz, 1H); ^{13}C NMR (CD$_3$CN) δ (ppm) 12.696 (q, $^2J_{B-C}$ = 165 Hz, B−CH$_3$), 45.484 (N−CH$_3$), 118.573, 121.509, 121.722, 125.589, 130.253, 130.479, 134.202, 135.875, 147.519, 149.472, 167.413 (q, $^2J_{B-C}$ = 194 Hz) (aromatic carbons). Elemental Anal. Calcd for C$_{29}$H$_{28}$BN (401.36): C, 86.78; H, 7.03; N, 3.49. Found: C, 86.92; H, 7.06; N, 3.53.

***N*-Methyl-3-cyanopyridinium methyltriphenylborate (10):** orange solid, 75% yield; ^{1}H NMR (CD$_3$CN) δ (ppm) 0.207 (q, $^2J_{B-H}$ = 3.9 Hz, 3H, B−CH$_3$), 4.125 (s, 3H, N−CH$_3$), 6.816 (t, J = 7.2 Hz, 3H, Ar−H of BPh$_3$), 6.977 (m, 6H, Ar−H of BPh$_3$), 7.234 (br, 6H, Ar−H of BPh$_3$), 7.983 (t, J = 8.4 Hz, 1H,

(31) (a) Hurd, D. T. *J. Org. Chem.* **1948**, *13*, 711. (b) Damico, R. *J. Org. Chem.* **1964**, *29*, 1971.

(32) Negishi, E.; Idacavage, M. J.; Chiu, K.-W.; Yoshida, T.; Abramovitch, A.; Goettel, M. E.; Silveria, A., Jr.; Bretherick, H. D. *J. Chem. Soc., Perkin Trans. 2* **1978**, 1225.

(33) Bockman, T. M.; Kochi, J. K. *J. Phys. Org. Chem.* **1997**, *10*, 542.

5-CH), 8.533 (d, $J = 8.4$ Hz, 1H, 4-CH), 8.645 (d, $J = 8.4$ Hz, 1H, 6-CH), 8.785 (s, 1H, 2-CH); ^{1}H NMR (THF-d_8) δ (ppm) 0.215 (q, $^2J_{B-H} = 4.2$ Hz, 3H, B−CH$_3$), 3.479 (br, 3H, N−CH$_3$), 6.689 (t, $J = 7.2$ Hz, 3H, Ar−H of BPh$_3$), 6.851 (t, $J = 7.2$ Hz, 6H, Ar−H of BPh$_3$), 7.321 (br, 6H, Ar−H of BPh$_3$), 7.55 (br, 1H, Ar−H), 8.0−8.40 (m, 3H, Ar−H); ^{13}C NMR (CD$_3$CN) δ (ppm) 12.686 (q, $^2J_{B-C} = 165$ Hz, B−Me), 49.003 (N−CH$_3$), 112.778, 113.628, 121.552, 125.648, 128.647, 132.788, 134.132, 148.389, 148.632, 167.096 (q, $^2J_{B-C} = 195$ Hz) (aromatic carbons). Elemental Anal. Calcd for C$_{26}$H$_{25}$BN$_2$ (451.42): C, 82.99; H, 6.70; N, 7.44. Found: C, 82.38; H, 6.78; N, 7.46.

N-Methylphenanthridinium methyltriphenylborate (11): yellow solid, 92% yield; ^{1}H NMR (THF-d_8) δ ppm 0.284 (q, $^2J_{B-H} = 4.2$ Hz, 3H, B−CH$_3$), 3.897 (s, 3H, N−CH$_3$), 6.532 (t, $J = 6.9$ Hz, 3H, Ar−H of BPh$_3$), 6.742 (t, $J = 7.2$ Hz, 6H, Ar−H of BPh$_3$), 7.330 (br, 6H, Ar−H of BPh$_3$), 7.90−8.20 (m, 5H, Ar−H), 8.262 (m, 1H, Ar−H), 8.468 (s, 1H, Ar−H), 8.87−9.00 (m, 2H, Ar−H); ^{13}C NMR (CD$_3$CN) δ (ppm) 12.664 (q, $^2J_{B-C} = 165$ Hz, B−Me), 45.959 (N−CH$_3$), 119.612, 121.498, 123.050, 124.634, 125.595, 130.488, 130.681, 132.129, 132.456, 134.192, 138.210, 155.071, 167.417(q, $^2J_{B-C} = 195$ Hz) (aromatic carbons). Elemental Anal. Calcd for C$_{33}$H$_{30}$BN (451.42): C, 87.80; H, 6.70; N, 3.10. Found: C, 87.55; H, 6.84; N, 3.16.

N-Methylacridinium methyltriphenylborate (12): brown yellow solid, 88% yield; ^{1}H NMR (CD$_3$CN) δ (ppm) 0.189 (q, $^2J_{B-H} = 3.9$ Hz, 3H, B−CH$_3$), 4.709 (s, 3H, N−CH$_3$), 6.799 (t, $J = 6.9$ Hz, 3H, Ar−H of BPh$_3$), 6.959 (m, 6H, Ar−H of BPh$_3$), 7.208 (br, 6H, Ar−H of BPh$_3$), 7.979 (m, 2H, Ar−H), 8.398 (m, 2H, Ar−H), 8.489 (m, 4H, Ar−H), 9.811 (s, 1H, 9-H); ^{13}C NMR (CD$_3$CN) δ (ppm) 12.664 (q, $^2J_{B-C} = 165$ Hz, B−Me), 38.297 (N−CH$_3$), 118.243, 121.455, 125.546, 126.598, 127.859, 131.708, 134.187, 139.277, 141. 638, 150.765, 167.089 (q, $^2J_{B-C} = 195$ Hz) (aromatic carbons). Elemental Anal. Calcd for C$_{33}$H$_{30}$BN (451.42): C, 87.80; H, 6.70; N, 3.10. Found: C, 85.17; H, 6.81; N, 5.64.

N-Methylisoquinolinium tetraphenylborate (13): white solid, 98% yield; ^{1}H NMR (CD$_3$CN) δ (ppm) 4.666 (s, 3H, N−CH$_3$), 6.748 (t, $J = 6.9$ Hz, 3H, Ph), 6.899 (t, 6H, $J = 6.9$ Hz, Ph), 7.337 (br, 6H, Ph), 8.050 (m, 1H), 8.242 (m, 3H), 8.278 (m, 2H), 9.292 (m, 1H); ^{13}C NMR (CD$_3$CN) δ (ppm) 46.048 (N−CH$_3$), 121.300, 125.120, 126.171, 127.477, 129.967, 131.521, 134.285, 135.428, 137.110, 148.495, 163.197 (q, $^2J_{B-C} = 195$ Hz) (aromatic carbons). Elemental Anal. Calcd for C$_{34}$H$_{30}$BN (363.43): C, 88.12; H, 6.52; N, 3.02. Found: C, 88.06; H, 6.53; N, 3.11.

N-Methylquinolinium tetraphenylborate (14): pale yellow solid, 98% yield; ^{1}H NMR (CD$_3$CN) δ (ppm) 4.356 (s, 3H, N−CH$_3$), 6.830 (t, $J = 6.9$ Hz, 4H, Ar−H of BPh$_3$), 6.993 (t, $J = 6.9$ Hz, 8H, Ar−H of BPh$_3$), 7.304 (br, 8H, Ar−H of BPh$_3$), 7.837 (t, $J = 5.7$ Hz, 1H), 7.988 (t, $J = 8.4$ Hz, 1H), 8.201 (m, 2H), 8.298 (d, $J = 8.4$ Hz, 1H), 8.707 (m, 1H), 8.951 (d, $J = 5.7$ Hz, 1H); ^{13}C NMR (CD$_3$CN) δ (ppm) 45.452 (N−CH$_3$), 118.551, 121.768, 125.613, 130.247, 130.490, 135.701, 135.843, 147.476, 149.409, 163.783 (q, $^2J_{B-C} = 195$ Hz) (aromatic carbons). Elemental Anal. Calcd for C$_{34}$H$_{30}$BN (363.43): C, 88.12; H, 6.52; N, 3.02. Found: C, 88.23; H, 6.60; N, 3.06.

N-Methyl-3-cyanopyridinium tetraphenylborate (15): yellow solid, 98% yield; ^{1}H NMR (CD$_3$CN) δ (ppm) 4.492 (s, 3H, N−CH$_3$), 6.748 (t, $J = 6.9$ Hz, 4H, Ar−H of BPh$_3$), 6.910 (m, 8H, Ar−H of BPh$_3$), 7.354 (br, 8H, Ar−H of BPh$_3$), 8.246 (t, $J = 8.4$ Hz, 1H, 5-CH), 8.978 (m, 2H, 4,6-CH), 9.374 (s, 1H, 2-CH); ^{13}C NMR (CD$_3$CN) δ (ppm) 49.121 (N−CH$_3$), 117.200, 121.358, 125.187, 128.765, 136.010, 148.334, 149.028, 149.286, 164.029 (q, $^2J_{B-C} = 195$ Hz) (aromatic carbons). Elemental Anal. Calcd for C$_{31}$H$_{27}$BN$_2$ (438.37): C, 84.94; H, 6.21; N, 6.39. Found: C, 84.84; H, 6.25; N, 6.47.

N-Methylphenanthridinium tetraphenylborate (16): pale yellow solid, 97% yield; ^{1}H NMR (CD$_3$CN) δ (ppm) 4.467 (s, 3H, N−CH$_3$), 6.818 (t, $J = 6.9$ Hz, 4H, Ar−H of BPh$_3$), 6.981 (t, $J = 6.9$ Hz, 8H, Ar−H of BPh$_3$), 7.291 (br, 8H, Ar−H of BPh$_3$), 8.0−8.2 (m, 3H), 8.3−8.5 (m, 3H), 8.85−9.0 (m, 2H),

9.425 (s, 1H); ^{13}C NMR (CD$_3$CN) δ (ppm) 45.985 (N−CH$_3$), 119.618, 121.728, 123.075, 123.687, 1124.599, 125.566, 125.983, 130.506, 130.683, 132.165, 132.454, 134.393, 135.007, 135.684, 138.148, 155.126, 163.763 (q, $^2J_{B-C} = 195$ Hz) (aromatic carbons). Elemental Anal. Calcd for C$_{38}$H$_{32}$BN (513.49): C, 88.89; H, 6.28; N, 2.73. Found: C, 89.02; H, 6.43; N, 2.71.

N-Methylacridinium tetraphenylborate (17): orange solid, 96% yield; ^{1}H NMR (CD$_3$CN) δ (ppm) 4.685 (s, 3H, N−CH$_3$), 6.825 (t, $J = 6.9$ Hz, 4H, Ar−H of BPh$_3$), 6.981 (t, $J = 6.9$ Hz, 8H, Ar−H of BPh$_3$), 7.276 (br, 8H, Ar−H of BPh$_3$), 7.974 (t, $J = 8.4$ Hz, 2H, Ar−H), 8.390 (t, $J = 8.4$ Hz, 2H, Ar−H), 8.492 (d, $J = 8.4$ Hz, 4H, Ar−H), 9.790 (s, 1H, 9-H); ^{13}C NMR(CD$_3$CN) δ (ppm) 38.397 (N−CH$_3$), 118.253, 121.717, 125.556, 126.608, 127.882, 131.713, 135.685, 139.292, 141. 645, 150.727, 162.759 (q, $^2J_{B-C} = 195$ Hz) (aromatic carbons). Elemental Anal. Calcd for C$_{38}$H$_{32}$BN (513.49): C, 88.89; H, 6.28; N, 2.73. Found: C, 88.93; H, 6.30; N, 2.65.

Tetrabutylammonium n-butyltrimethylborate (18): ^{1}H NMR (CD$_3$CN) δ (ppm) −0.742 (q, $^2J_{B-H} = 3.9$ Hz, 9H, B-Me), −0.155 (m, 2H, B−CH$_2$), 0.835 (t, $J = 7.2$ Hz, 3H), 0.968 (t, $J = 7.2$ Hz, 12H), 1.050 (m, 2H), 1.176 (m, 2H), 1.350 (m, 8H), 1.600 (m, 8H), 3.079 (t, $J = 9.0$ Hz, 8H, N−CH$_2$).

Tetramethylammonium sec-butyltri(n-butyl)borate (19): ^{1}H NMR (THF-d_8) δ (ppm) −0.30 (m, 7H, B−CH$_2$ and B−CH), 0.6−0.85 (m, 15H, CH$_3$), 1.00−1.20 (m, 14H, CH$_2$), 3.42 (s, 3H, N−CH$_3$).

Thermal Decomposition of [Py$^+$BR$_4^-$] in THF. The general procedure was described as follows using [**iQ**$^+$BMe$_4^-$] as an example: 200 mg (0.93 mmol) of [**iQ**$^+$BMe$_4^-$] was dissolved in 10 mL of THF at room temperature and stirred for 1 h. The solvent was pumped out and condensed into a flask containing NH$_3$. The residue was purified and identified as 1,2-dihydro-1,2-dimethylisoquinoline[34] by ^{1}H NMR (yield: 142 mg, 96%). The flask containing volatile was warmed to −30 °C, and the solvent and excess NH$_3$ were removed at this temperature to give a crystalline solid, which melted at room temperature and was identified as a 1:1 mixture of Me$_3$B-(NH$_3$)[35] (68% yield) and THF. ^{1}H NMR (CD$_3$CN): δ (ppm) −0.435 (s, 9H, BMe$_3$), 1.804 (m, 4H, THF), 3.182 (br, 3H, NH$_3$), 3.623 (m, 4H, THF). The results of the other [**Py**$^+$BR$_4^-$] salts are presented in Table 3.

Decomposition of [mP$^+$BMe$_4^-$] (7) in the Solid State. A solid sample of [**mP**$^+$BMe$_4^-$] (185 mg, 0.70 mmol) was charged in a Schlenk flask; the flask was then closed and kept at room temperature for 1 day. The gas formed was condensed at −196 °C into a flask containing NH$_3$ (dried by sodium). The residue was purified and identified as 9,10-dihydro-9,10-dimethylphenanthridine by ^{1}H NMR (yield: 145 mg, 99%). The flask containing volatile was warmed to −78 °C, and the excess NH$_3$ was removed at this temperature to give a crystalline solid which was identified as Me$_3$B(NH$_3$)[35] (39 mg, 76% yield).

Decomposition of N-Methylisoquinolinium n-Butyltrimethylborate in THF at Low Temperature. N-Methylisoquinolinium n-butyltrimethylborate was prepared in situ by treating 355 mg (1.0 mmol) of tetrabutylammonium n-butyltrimethylborate with 293 mg (1.0 mmol) of N-methylisoquinolinium triflate in 20 mL of THF at −78 °C. After the mixture was warmed to 0 °C in 3 h, the volatile was removed in vacuo. From the residue a mixture of 1,2-dihydro-1-butyl-2-methylisoquinoline and 1,2-dihydro-1,2-dimethylisoquinoline was isolated by chromatographing on a small silica column (180 mg). The ratio of these products was determined by the ^{1}H NMR signal of N−CH$_3$. Decomposition of N-methylisoquinolinium s-butyltri(n-butyl)borate, N-methylquinolinium tetramethylborate, and 3-cyano-N-methylpyridinium tetramethylborate at low temperature followed a similar procedure, and the results are presented in Tables 5 and 6.

(34) (a) Kitane, S.; Tshiamala, K.; Laude, B.; Vebrel, J.; Ceratti, E. *Tetrahedron* **1985**, *42*, 3737. (b) See ref 19b.
(35) Heitsch, C. H. *Inorg. Chem.* **1964**, *4*, 1019.

Photoactivation of the Charge-Transfer Salts in Solution. The general procedure is described as follows using [**iQ**⁺BMePh₃⁻] as an example: 150 mg (0.37 mmol) of [**iQ**⁺BMePh₃⁻] was dissolved in THF and irradiated using a mercury lamp with a cutoff filter (>370 nm) for 3 h. The solvent was removed and the residue was separated by TLC (methylene chloride as eluent) to give 32 mg of 1,2-dimethyl-1,2-dihydroisoquinoline (54% yield), which was identified by ¹H NMR. The results of the other charge-transfer salts are summarized in Table 4.

Photoactivation of [Q⁺BMe₄⁻] in THF at −78 °C. A solid sample of [**Q**⁺BMe₄⁻] (35.0 mg, 0.16 mmol) was dissolved in 2 mL of THF at −78 °C. The resulting solution was irradiated using a mercury lamp with a cutoff filter (>370 nm) at −78 °C for 1 h. Cold pentane (5 mL) was added at −78 °C, and no precipitate was formed. (In the control experiment, addition of cold pentane resulted in the precipitation of yellow [**Q**⁺BMe₄⁻], which was separated from the solution via filtration at −78 °C. No methyl-transfer product was obtained from the resulting solution.) All the volatile was removed to give an orange oil (25 mg, total yield 98%), which was spectroscopically identified as a mixture of 1,2-dihydro-1,2-dimethylquinoline and 1,4-dihydro-1,4-dimethylquinoline. The ratio of these products was determined by ¹H NMR signals of 2-CH₃ in the 1,2-isomer and 4-CH₃ in the 1,4-isomer.

Photoactivation of N-Methylisoquinolinium n-Butyltrimethylborate in THF at −78 °C. N-Methylisoquinolinium n-butyltrimethylborate was prepared in situ by treating 71.0 mg (0.20 mmol) of tetrabutylammonium n-butyltrimethylborate with 58.6 mg (0.20 mmol) of N-methylisoquinolinium triflate in 4 mL of THF and 0.2 mL of acetonitrile at −78 °C. A procedure similar to that above was then followed, and the result is presented in Table 6.

Photoactivation of the Charge-Transfer Salts in the Solid State. The general procedure was described as follows using [**iQ**⁺BMe₄⁻] as an example: A powder sample of [**iQ**⁺BMe₄⁻] (3.6 mg) in a NMR tube was irradiated using a mercury lamp with a cutoff filter (>370 nm) for 5 h. The yellow solid sample changed to an orange liquid. The yield (71%) of 1,2-dimethyl-1,2-dihydroisoquinoline was determined by ¹H NMR using toluene as an internal standard. The results of the other charge-transfer salts are summarized in Table 7.

X-ray Crystallography.[36] The cell dimensions and diffraction intensities of [**iQ**⁺,BMe₄⁻], [**iQ**⁺,BMePh₃⁻], and [**NCP**⁺,BPh₄⁻] were measured at −150 °C with a Siemens SMART diffractometer equipped with a CCD detector and an LT-2 low-temperature device. The data were collected with graphite-monochromatized Mo Kα radiation (λ = 0.710 73 Å) using an ω-scan technique over a hemisphere of the reciprocal space. The usual Lorentz and polarization corrections were made. The decay and absorption corrections have been considered to be negligible for the crystals investigated. All the structures were solved by direct methods[37] and refined by full-matrix least-squares on F^2 in anisotropic approximation for all nonhydrogen atoms (Table 8).[38] In the structure of [**NCP**⁺,BPh₄⁻] shown in Figures 6 and 7, where both the cation and the anion occupy the special crystallographic position of the *mm*2 symmetry, the resulting disorder of the cation and two approaching phenyl groups of the anion was successfully resolved using a

Table 8. Crystallographic Data and Details of Refinements for the Charge-Transfer Salts

	[iQ⁺,BMe₄⁻]	[iQ⁺,BMePh₃⁻]	[NCP⁺,BPh₄⁻]
formula	$C_{14}H_{22}BN$	$C_{29}H_{28}BN$	$C_{31}H_{27}BN_2$
fw, g mol⁻¹	215.14	401.33	438.36
cryst syst	triclinic	triclinic	orthorhombic
space group	$P\bar{1}$	$P\bar{1}$	*Cmcm*
a, Å	7.5564(4)	10.2317(1)	9.850(7)
b, Å	8.9451(5)	10.6679(1)	15.70(2)
c, Å	11.5968(6)	11.8138(1)	14.87(1)
α, deg	85.028(1)	69.979(1)	90
β, deg	77.458(1)	70.362(1)	90
γ, deg	67.023(1)	70.100(1)	90
V, Å³	704.45(7)	1103.48(2)	2300(4)
Z	2	2	4
cryst size, mm	0.8 × 0.7 × 0.3	0.3 × 0.3 × 0.1	0.5 × 0.4 × 0.15
$F(000)$	236	428	928
D_c, g cm⁻³	1.014	1.208	1.266
μ(Mo Kα), mm⁻¹	0.057	0.068	0.073
2θ range, deg	3.6−65.0	3.8−66.0	4.8−60.0
h_{min}, h_{max}	0, 10	−13, 14	0, 14
k_{min}, k_{max}	−12, 13	−14, 15	0, 21
l_{min}, l_{max}	−16, 12	0, 17	0, 22
no. of measd reflns	6286	10618	4396
no. of ind reflns	4399	7239	1751
R_{int}	0.0255	0.0568	0.0856
no. of obsd reflns[a]	3687	5687	954
total no. of variables	233	282	137
R[b]	0.0504	0.0536	0.0726
R_w[c]	0.1352	0.1335	0.1355
S[d]	1.083	1.042	1.084
extinction param x			0.010(2)
$\Delta\rho_{max}/\Delta\rho_{min}$, e Å⁻³	0.390/ −0.209	0.371/ −0.304	0.501/ −0.207

[a] With $I > 2.0s(I)$. [b] $R = \sum||F_o| - |F_c||/\sum|F_o|$. [c] $R_w = \{\sum[w(F_o^2 - F_c^2)^2]/\sum[w(F_o^2)^2]\}^{1/2}$. [d] $S = \{\sum[w(F_o^2 - F_c^2)^2]/\sum(N - n)\}^{1/2}$. [e] Multiplying the overall scale factor by $[1 + 0.001xF_c^2\lambda^3/\sin(2\theta)]^{-1/4}$.

series of difference Fourier syntheses.[39] All the hydrogen atoms in the structures of [**iQ**⁺,BMe₄⁻] and [**iQ**⁺,BMePh₃⁻] were put in geometrically calculated positions and refined using a riding/rotating model[38] with the isotropic temperature factors constrained to $U_{iso}(H) = 1.2U_{eq}(C)$ of the adjacent carbon atom; in the structure [**NCP**⁺,BPh₄⁻], both positional and isotropic temperature parameters of the hydrogens were refined independently.

Supporting Information Available: Tables of crystal-structure data for [**iQ**⁺,BMe₄⁻]. [**iQ**⁺,BMePh₃⁻], and [**NCP**⁺,-BPh₄⁻] including atomic coordinates, anisotropic thermal parameters, bond lengths/angles, hydrogen coordinates, and least-squares planes (14 pages). Ordering information is given on any current masthead page.

OM9808054

(36) Atomic coordinates for the structures of [**iQ**⁺,BMe₄⁻], [**iQ**⁺,-BMePh₃⁻], and [**NCP**⁺,BPh₄⁻] have been deposited with the Cambridge Crystallographic Data Centre. They can be obtained, upon request, from the Director, Cambridge Crystallographic Data Centre, 12 Union Road, Cambridge, CB2 1eZ, U.K.

(37) Sheldrick, G. M. *SHELXS86*, Program for the Solution of Crystal Structures; University of Göttingen, Germany, 1985.

(38) Sheldrick, G. M. *SHELXL93*, Program for the Refinement of Crystal Structures; University of Göttingen, Germany, 1993.

(39) Attempts to solve the structure in noncentrosymmetric space group *Cmc*2₁ resulted in the same kind of disorder. Since the disorder did not result from the proper symmetry choice, the crystal can be a centrosymmetric twin of two chiral components (which we also considered). The refinement in the centrosymmetric space group *Cmcm* provided the best precision relative to noncentrosymmetric and twinned models.